

## THE PHASE SEPARATION PHENOMENOLOGICAL MODEL: MANGANITE AS AN EXAMPLE

T.S. Shaposhnikova, R.F. Mamin

Zavoisky Physical-Technical Institute, FRC KazanSC of RAS, Kazan, Russian Federation

In the paper, an effect of a second order phase transition has been considered in the context of the phenomenological model for a 2D charged system (2DCS) frustrated by the Coulomb interaction. The relationship between the order parameter and the charge was treated as a local temperature in the 2DCS. The existence of phase-separated states was shown to be a possibility in such a system. Various types of those states (strips, rings, etc.) were found by numerical calculations, and their parameters were determined. As the temperature is lowered, the 2DCS passes several phase transitions successively. Using the  $\text{La}(1-x)\text{Sr}(x)\text{MnO}_3$  manganite as an example it was shown that such a phenomenological model could be used to describe the phase separation close to a magnetic phase transition from a ferromagnetic state to a paramagnetic one when  $0.10 < x < 0.15$  and at the temperatures of  $100 < T < 200$  K.

**Key words:** second order phase transition, phase separation, manganite, Coulomb interaction, doping level

**Citation:** T.S. Shaposhnikova, R.F. Mamin, The phase separation phenomenological model: Manganite as an example, St. Petersburg Polytechnical State University Journal. Physics and Mathematics. 11 (3) (2018) 11–18. DOI: 10.18721/JPM.11302

### Introduction

The problem of phase separation has attracted much attention from researchers [1 – 8]. There are two classes of materials where phase transitions (PT) are observed with various types of structural, magnetic, charge, and orbital ordering.

The first class is manganites with colossal negative magnetoresistance of the  $R_{1-x}A_x\text{MnO}_3$  type ( $R = \text{La, Pr, Sm, etc.}, A = \text{Ca, Sr, etc.}$ ), whose physical properties are greatly affected by the concentration  $x$  of the divalent element  $A$  varying from zero to unity [1 – 5, 8].

The second class are high-temperature cuprate superconductors, where a pseudo-gap state and charge-density waves are observed [6, 7].

Phase separation of substances is often accompanied by charge inhomogeneities. Such inhomogeneities were observed by scanning tunneling microscopy [9], angle-resolved photoemission spectroscopy (ARPES) [6], X-ray and neutron diffraction [7]. For the above-mentioned compounds, there is a certain range of temperatures and doping levels for which the ground energy state corresponds to phase coexistence. The spatial size of single-phase regions depends on the ratio between the Coulomb en-

ergy (important in the presence of a doping-induced overcharge) and the energy gain due to the presence of a more ordered phase [10, 11]. States with charge inhomogeneity have been the focus of many theoretical studies (see, for example, Refs. [12 – 15]), usually considering a first-order phase transition frustrated by the Coulomb interaction. The scalar order parameter for this type of PT is either linearly coupled with charge density or proportional to it [13, 14]. These studies have established that such models are unstable with respect to phase separation. The phase-separated state is a group of charged regions of different phases with different values of the order parameter. Notably, this type of coupling of the order parameter to charge density is forbidden in case of a second-order phase transition and the order parameter is not a scalar quantity.

In this study, we discuss a second-order PT frustrated by the Coulomb interaction. We have considered the coupling between the charge density and the squared order parameter. We have established within the framework of this model that a phase-separated state with charge inhomogeneities can exist near the phase transition temperature  $T_c$ , where the high-temperature phase matrix with an order parameter equal to  $\eta_1$  contains inclusions of a

low-temperature phase with an order parameter  $\eta_2 > \eta_1$ . Several successive first and second-order PTs can be observed with a change in the temperature.

We have applied the phenomenological approximation, based on the Ginzburg – Landau theory, to describe static phase separation in a two-dimensional system in the vicinity of a second-order phase transition. In this case, the presence of the Coulomb interaction associated with doping-induced overcharging is taken into account. Since the above-mentioned materials are quasi-two-dimensional (CuO planes in cuprates and MnO planes in manganites), the two-dimensional description adopted is a reasonable approximation. We have defined a set of parameters, related to temperature and doping, for which phase separation is energetically favorable. We have also found the region of the phase diagram where the inhomogeneous phases coexist.

We have calculated the model parameters suitable for describing phase separation near the magnetic PT of the second order in  $\text{La}_{1-x}\text{Sr}_x\text{MnO}_3$  with  $0.10 < x < 0.15$ .

### Theoretical model

Let us consider a two-dimensional system near a second-order phase transition. A study by Nobel Prize winner Pierre-Gilles de Gennes [16] investigated the effect of double exchange in mixed-valence compounds such as manganites  $(\text{La}_{1-x}\text{Ca}_x)(\text{Mn}_{1-x}^{3+}\text{Mn}_x^{4+})\text{O}_3$ . It was established that introducing extra holes or extra electrons into the antiferromagnet lowered the energy of the system. Additionally, the Curie temperature was found to depend on the doping level  $x$ . Following de Gennes's study, we start with a Hamiltonian, adding to it a term with the Coulomb interaction. The Hamiltonian for a "layer" antiferromagnet can be written in the following form:

$$H = -\sum_{ij} J_{ij} \mathbf{S}_i \cdot \mathbf{S}_j - \sum_{ij\sigma} t_{ij} a_{i\sigma}^+ a_{j\sigma} - J_H \sum_i \mathbf{S}_i \cdot \mathbf{s}_i + H_{\text{Coul}}. \quad (1)$$

The first term in this expression describes the exchange interaction of Mn ions;  $\mathbf{S}_i, \mathbf{S}_j$  are the spin operators of ionic spin at sites  $i$  and  $j$ ;  $J_{ij}$  is the exchange integral (connecting only

neighboring magnetic sites  $i$  and  $j$ ); the second and third terms of Hamiltonian (1) describe a double exchange: the second term describes the jumps of an electron with spin  $\sigma$  along the  $ij$  sites of the lattice;  $a_{i\sigma}^+$  ( $a_{i\sigma}$ ) is the creation (annihilation) operator for an electron at site  $i$ ;  $t_{ij}$  is the hopping integral; the third term in Hamiltonian (1) describes Hund's coupling [17],  $\mathbf{s}_i$  is the spin operator of the conduction electron (it can be expressed in terms of the creation and annihilation operators for the electron and the Pauli matrices); the last term describes the Coulomb interaction.

Following de Gennes, we have assumed that spin ordering of an unperturbed system is of the "antiferromagnetic layer" type. Each ionic spin  $S$  is ferromagnetically coupled to  $z'$  neighboring spins the same layer and antiferromagnetically to  $z$  spins in the neighboring layers. The exchange integrals are equal to  $t_{ij}'$  and  $t_{ij}$ , respectively. Zener charge carriers [18] hop within their layer (with the hopping integral  $t_{ij}'$ ) and from one layer to another (with the hopping integral  $t_{ij}$ ).

Let the number of magnetic ions per unit volume of the sample be equal to  $N$  and the number of Zener carriers to  $xN$ . The model of double exchange is a model of exchange under the conditions of strong coupling  $J_H \gg zt, z't'$ .

A phenomenological expression for free energy was derived in [16] in the finite temperature limit and for low values of relative sublattice magnetizations.

The density of the thermodynamic potential of the system in the strong coupling limit  $J_H \rightarrow \infty$  then takes the form

$$\phi(\eta, \rho) = \phi_0 + \phi_\eta + \phi_{int} + \phi_{\text{Coul}}, \quad (2)$$

while for a second-order PT, the second term should be expressed as

$$\phi_\eta = \frac{\alpha}{2} \eta^2 + \frac{\beta}{4} \eta^4 + \frac{\delta}{6} \eta^6 + \frac{\zeta}{8} \eta^8 + \frac{D}{2} (\nabla \eta)^2, \quad (3)$$

where the order parameter  $\eta$  describes the relative magnetization of each sublattice;

$$\alpha = \alpha'(T - T_c)$$

( $T_c$  is the PT temperature without doping).

Expression (3) contains a second-order term with respect to  $\eta$ , positive terms of the

fourth, sixth and eighth orders with respect to  $\eta$  and a gradient term. In addition, expression (3) includes constants

$$\alpha = 2N(1,5k_B T - S^2(zJ + z'J')), \quad (4)$$

$$\beta = 4N(0,45k_B T + 0,034x(zt + z't')); \quad (5)$$

$$\delta = 6N(0,325k_B T + 0,27x(zt + z't')); \quad (6)$$

$$\zeta = 8N(0,06k_B T + 2,21x(zt + z't')), \quad (7)$$

where  $k_B$  is the Boltzmann constant.

The energy  $\phi_{int}$  in function (2) describes the interaction of the order parameter  $\eta$  with the local charge density  $\rho$ :

$$\phi_{int} = -\frac{\sigma_1}{2}\eta^2\rho. \quad (8)$$

This formula is obtained from the temperature-averaged terms of expression (1) describing the double exchange. The interaction energy (8) is written in this case as a local temperature;  $\sigma_1$  is the constant of this interaction.

The main physical properties of the system are determined by the parameter  $\sigma_1$ , found from the following expression:

$$\bar{\rho}\sigma_1 = \frac{4N}{5}x(zt + z't'). \quad (9)$$

The energy of the Coulomb interaction  $\phi_{Coul}$  is expressed by the integral:

$$\phi_{Coul} = \frac{\gamma}{2} \int \frac{(\rho(\mathbf{r}) - \bar{\rho})(\rho(\mathbf{r}') - \bar{\rho})}{|\mathbf{r} - \mathbf{r}'|} d\mathbf{r}', \quad (10)$$

where the constant  $\gamma$  is the dielectric constant of the medium.

In the absence of the  $\phi_{int}$  and  $\phi_{Coul}$  terms, a second-order PT is observed at  $\alpha = 0$ . There is an equilibrium value of the order parameter for  $\alpha = 0$ . For  $\alpha < 0$ , the equilibrium value of the order parameter  $\eta = 0$ , i.e., there is no order which can be determined by the parameter  $\eta$ .

In expressions (9) and (10),  $\bar{\rho}$  is the mean 2D surface charge density:

$$\bar{\rho} = \frac{1}{S} \int_S \rho d^2\mathbf{r}, \quad (11)$$

where  $\mathbf{r}$  is a two-dimensional vector.

The total free energy  $\Phi$ , which is expressed as

$$\Phi = \int \phi(\eta, \rho) d^2\mathbf{r}, \quad (12)$$

should be minimized with respect to  $\eta$  and  $\rho$ .

Minimizing the energy  $\Phi$  with respect to the local charge density  $\rho$  yields the equality

$$-\frac{\sigma_1}{2}\nabla_{3D}^2\eta^2 = 4\pi\gamma(\rho(\mathbf{r}) - \bar{\rho})\delta(z)d. \quad (13)$$

The thickness of the two-dimensional layer  $d$  is introduced to preserve the dimensionality;  $\delta(z)$  is the Dirac delta function

Substituting (13) into expression (2), we obtain

$$\begin{aligned} \phi = & \phi_0 + \frac{\alpha}{2}\eta^2 + \frac{\beta}{4}\eta^4 + \\ & + \frac{\delta}{6}\eta^6 + \frac{\zeta}{8}\eta^8 + \frac{D}{2}(\nabla\eta)^2 - \frac{\sigma_1}{2}\eta^2\bar{\rho} - \\ & - \frac{\sigma_1^2}{32\pi^2\gamma d^2} \int \frac{\nabla_{2D}\eta^2(\mathbf{r})\nabla_{2D}\eta^2(\mathbf{r}')}{|\mathbf{r} - \mathbf{r}'|} d\mathbf{r}', \end{aligned} \quad (14)$$

where  $\mathbf{r}, \mathbf{r}'$  are two-dimensional vectors.

The last two terms in expression (14) are negative. The term  $-(\sigma_1/2)\eta^2\bar{\rho}$  renormalizes the critical temperature of the phase transition that now becomes dependent on the mean charge density.

The coefficient before the parameter  $\eta^2$  should now be changed (to  $\tilde{\alpha}$  instead of  $\alpha$ ):

$$\tilde{\alpha} = \alpha - \sigma_1\bar{\rho}. \quad (15)$$

Notably, the presence of the last non-local term in expression (14) leads to instability of the homogeneous state.

Let us introduce dimensionless parameters  $\Lambda$  and  $\xi$  as

$$\Lambda = \eta / \eta_0; \quad \xi_x = x / a; \quad \xi_y = y / a,$$

where  $\eta_0^4 = \beta / \zeta$ ,  $a = [D\zeta^{1/2} / (2\beta^{3/2})]^{1/2}\chi$  ( $\chi$  is a constant, the expressions for the constants  $\beta$  and  $\zeta$  are given by formulae (5) and (7)).

We chose the value of the constant  $\chi$  in the interval from 3 to 20. This allowed to vary the size of the region where the spatial distribution of the order parameter was calculated.

Expression (14) then takes the following form:

$$\begin{aligned} \phi = & U_0(\tau\Lambda^2 + \frac{\Lambda^4}{2} + \tilde{\delta}\frac{\Lambda^6}{3} + \frac{\Lambda^8}{4} + \frac{2}{\chi^2}(\nabla\Lambda)^2 - \\ & - \frac{A}{\chi} \int \frac{\nabla_{2D}\Lambda^2(\xi)\nabla_{2D}\Lambda^2(\xi')}{|\xi - \xi'|} d\xi'. \end{aligned} \quad (16)$$

The parameters  $U_0$ ,  $\tau, \chi$ ,  $A$  and  $\tilde{\delta}$  in this expression are defined as follows:

$$U_0 = \frac{\beta}{2} \eta_0^4 = \frac{\beta^2}{2\zeta}, \quad (17)$$

$$\tau = \frac{\tilde{\alpha}}{\beta \eta_0^2} = \sqrt{\frac{\zeta}{\beta^3}} \alpha' \left( T - T_c - \frac{\sigma_1 \bar{\rho}}{\alpha'} \right), \quad (18)$$

$$\chi = a \eta_0 \sqrt{\frac{2\beta}{D}}, \quad (19)$$

$$A = \frac{\sigma_1^2}{8\gamma d^2 \pi^2 \sqrt{2D} \sqrt{\beta\zeta}}, \quad (20)$$

$$\tilde{\delta} = \frac{\delta}{\beta} \eta_0^2 = \frac{2\delta}{\sqrt{\beta\zeta}}. \quad (21)$$

### Calculation results and discussion

To find the minimum of the free energy (12), we applied the conjugated gradient method (CGM). We introduced  $N \times N$  ( $N = 128$ ) discrete points on a square with a side  $a$  and applied periodic boundary conditions. Three parameters  $A$ ,  $\tau$  and  $\chi$  were taken in the calculations.

We analyzed the dependence of the free energy on the parameters  $A$  and  $\tau$  for a fixed value of the constant  $\chi$ .

Fig. 1, *a* shows the spatial distribution of the order parameter  $\Lambda = \Lambda(\xi_x, \xi_y)$  for the parameter values  $A = 2.5$ ,  $\tau = 0.6$ ,  $\chi = 10$ , and

$N = 128$ . Phase separation can be observed at these values. For a homogeneous background with an order parameter equal to zero (see the scale on the right), there is a ring with a non-zero order parameter, i.e.,

$$0 < \Lambda(\xi_x, \xi_y) \leq 1.8.$$

The free energy is negative in this state ( $\Phi < 0$ ). This means that the spatially inhomogeneous distribution of the order parameter corresponds to minimal free energy. This state is more energetically favorable than the homogeneous one whose free energy is zero ( $\Phi = 0$  for  $\Lambda(\xi_x, \xi_y) = 0$ ). Such inhomogeneous states are formed due to charge redistribution. A triple extra-charged layer exists in the region where the parameter  $\Lambda(\xi_x, \xi_y)$  is distributed inhomogeneously. The total charge in this layer is equal to zero with high accuracy,  $\Delta\rho > 0$  in the center of the stripe and  $\Delta\rho < 0$  on each side.

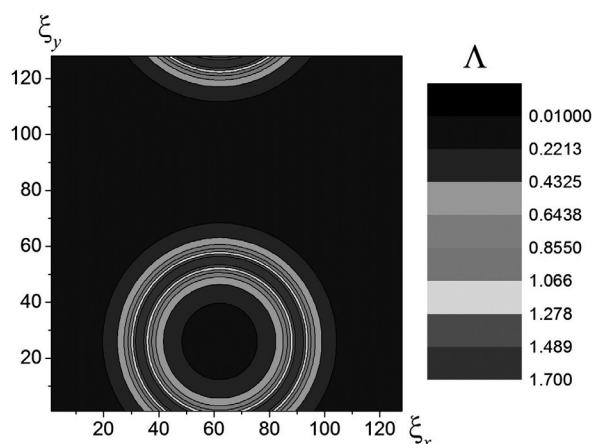
For a fixed value of the parameter  $A = 2.5$ , the inhomogeneous distribution of the order parameter exists for the values of the parameter  $\tau$  lying in the range

$$\tau_2 \leq \tau \leq \tau_3$$

( $\tau_2 = -9$  and  $\tau_3 = 1.5$ ).

The free energy is less than zero for the region  $\tau \leq \tau_1$  ( $\tau_1 = 0.8$  for  $A = 2.5$ ). In accordance with expression (18),  $\tau$  is a linear function of the difference  $T - T_c$  and varies depending on

*a)*



*b)*

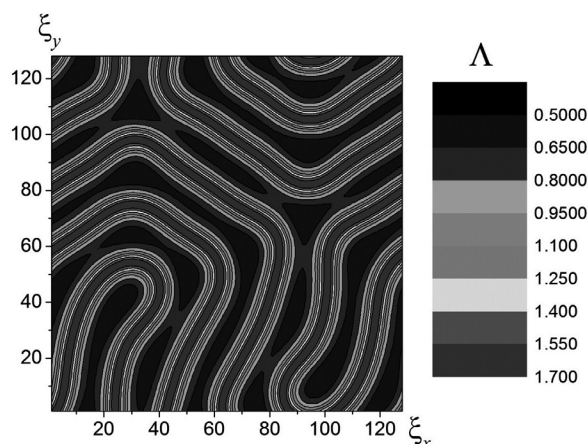


Fig. 1. Calculated distributions of the order parameter  $\Lambda(\xi_x, \xi_y)$  in the inhomogeneous state for  $\tau = 0.6$  (*a*) and  $-3.0$  (*b*);  $A = 2.5$ ,  $\chi = 10$ . The number of discrete points  $N^2 = 128^2 = 16384$

$\bar{\rho}$ . Here,  $T_c$  is the temperature of the phase transition without interaction (i.e., for  $\Phi_{int} = 0$ );  $\bar{\rho}$  is the value of the mean charge proportional to the doping level. The parameter  $A$  (see Eq. (20)) depends on the coupling parameter  $\sigma_1$  and on the strength of the Coulomb interaction. As the latter increases, the parameter  $A$  decreases. This shortens the interval of  $\tau$  values where phase separation can be observed.

Fig. 1,*b* shows the inhomogeneous distribution of the order parameter  $\Lambda(\xi_x, \xi_y)$  for the parameter values  $A = 2.5$ ,  $\tau = -3, 0$ ,  $\chi = 10$  ( $N = 128$ ). The order parameter varies from  $\Lambda_{min} = 0.5$  to  $\Lambda_{max} = 1.7$  (see the scale on the right). An inhomogeneous distribution of the extra charge exists in the region where the order parameter  $\Lambda$  is distributed inhomogeneously. Calculations show that varying the parameter  $\chi$  from 3 to 20 (with  $A = \text{const}$ ) does not affect the interval of  $\tau$  values where inhomogeneous states are formed.

Fig. 1 illustrates how the phase separation landscape changes with the changing  $\tau$ . Phase separation is observed in the form of stripes or rings for  $\tau > 0$  (see Fig. 1,*a*). A stripe with  $\Lambda > 0$  appears on the background with a zero order parameter  $\Lambda = 0$ . The stripes may be straight or have a complex closed form. The number of such stripes decreases with increasing  $\tau$ , and the rings are compressed. Notably, the order parameter value does not change at the center of these stripes. The shapes of the loops change as the value of  $\tau$  becomes negative (see Fig. 1,*b*) and with a further decrease in  $\tau$ : the loops bend more, and the order parameter value in the “background” becomes different from zero ( $\Lambda_{min} = 0.5$  in Fig. 1,*b*). Phase separation becomes shallower with a further decrease in  $\tau$  (these data are not shown in Fig. 1). The difference between the  $\Lambda$  value inside and outside the “stripes” drops to zero at  $\tau = \tau_2$ , and a transition to a homogeneous state with  $\Lambda = \text{const}$  is observed.

Our model includes the interaction of the order parameter with the charge ( $\sigma_1 \neq 0$ ). In the presence of this interaction, an inhomogeneous phase-separated state with the order parameter varying from  $\Lambda_{min}$  to  $\Lambda_{max}$  (see Fig. 1,*b*) has a minimal negative free energy  $\Phi_{inhom} < 0$ .

Let us consider the change of phases observed with decreasing  $\tau$  and at a constant

value of  $A = 2.5$ . The inhomogeneous phase state appears abruptly (a second-order PT) at  $\tau = \tau_1 = 0.8$ . Stripes with  $\Lambda \neq 0$  grow on the “background” with a zero order parameter  $\Lambda = 0$ . In these stripes,  $\Lambda_{max} = 1.8$ . The number of such stripes increases as  $\tau$  decreases from  $\tau_1$  to 0. Notably, the values  $\Lambda_{max} = 1.8$  and  $\Lambda_{min} = 0$  do not change in this region of  $\tau$ . The phase-separated state starts to change at  $\tau = 0$ :  $\Lambda_{max}$  starts to decrease and  $\Lambda_{min}$  to increase. With further decrease of  $\tau < 0$ , the difference between  $\Lambda_{max}$  and  $\Lambda_{min}$  decreases and  $\Lambda_{max} = \Lambda_{min} = \Lambda$  when  $\tau = \tau_2 = -9$ , i.e., a second-order PT from an inhomogeneous to a homogeneous state is observed. In this case, the energy of the inhomogeneous state  $\Phi_{inhom} < 0$  is less than the energy of the homogeneous state  $\Phi_{hom}$  (this state exists in the absence of interaction between the order parameter and the charge, i.e., with  $\sigma_1 = 0$ ) for the entire range of values of the parameter  $\tau_2 < \tau < \tau_1$ .

The phase diagram of inhomogeneous states in Fig. 2 is shown in the axes  $1/A - T$  ( $T$  is the temperature), for which  $\Delta\Phi < 0$ , i.e., the energy of the inhomogeneous

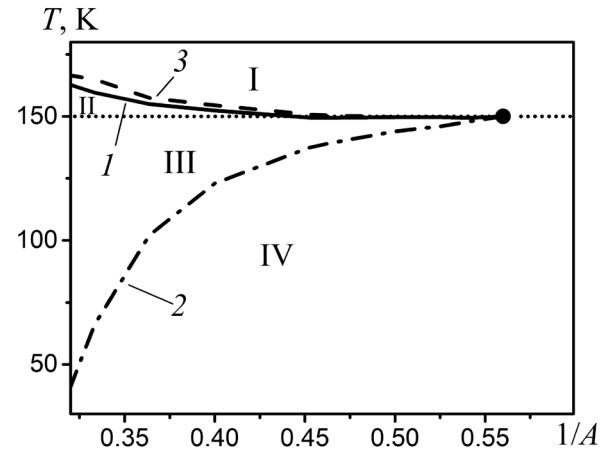


Fig. 2. Phase diagram of inhomogeneous states in  $1/A - T$  axes ( $T$  is the temperature): region I corresponds to a homogeneous non-magnetic state, regions II and III correspond to a phase-separated state, region IV corresponds to a homogeneous magnetic state;  $\Lambda = 0$  in region I;  $\Lambda = 0$  and  $\Lambda \neq 0$  in region II,  $\Lambda \neq 0$  in regions III and IV. The parameters used are given in the text. The boundaries of the regions are  $T = f_1(\tau_1)$  (curve 1),  $T = f_2(\tau_2)$  (2),  $T = f_3(\tau_3)$  (3);  $1/A = 0.555$  is the final critical point; if  $1/A > 0.555$ , phase separation is impossible

phase-separated state  $\Phi_{inhom}$  is less than the energy of the homogeneous state  $\Phi_{hom}$  at  $\tau_2 < \tau < \tau_1$ . The difference  $\Delta\Phi = \Phi_{hom} - \Phi_{inhom}$ . The following parameters were used:

$$T_c + \frac{\sigma_1 \bar{\rho}}{\alpha'} = 150 \text{ K}; \quad \frac{\tau}{\alpha'} \sqrt{\frac{\beta^3}{\zeta}} = 3 \text{ K}.$$

Regions I and IV correspond to homogeneous phases with zero and nonzero order parameters, respectively. Regions II and III correspond to inhomogeneous phases. The value of  $1/A$  is directly proportional to the value of the Coulomb interaction  $\gamma$  and inversely proportional to the square  $\sigma_1$  (see expression (20)). As the parameter  $A$  decreases ( $1/A$  increases), the interval of  $\tau$  values narrows, and, consequently, so does the temperature range  $T(\tau)$ , where the inhomogeneous distribution of the order parameter  $\Lambda$  is observed. Phase separation is impossible below the critical end point  $A = 1.8$  ( $1/A = 0.555$ ), which is shown in the phase diagram in Fig. 2. Indeed, with a high value of the Coulomb interaction and a low value of the double exchange energy, the Coulomb energy for charge modulation of the charge becomes so large that it is always greater than the energy gain associated with ordering.

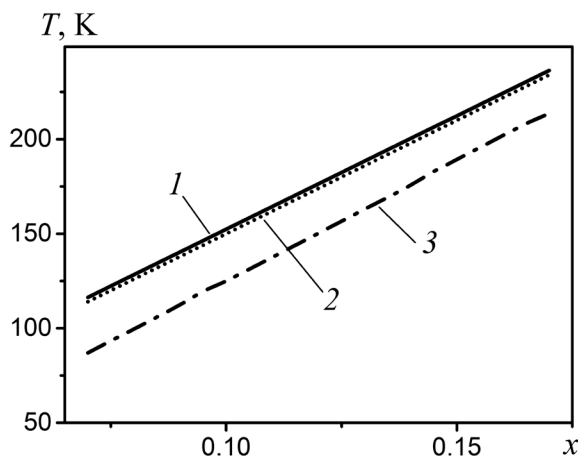


Fig. 3. Phase diagram in  $x - T$  axes for different values of the parameter  $\tau$  (the rest of the parameters used are given in the text). The region between lines 1 and 3 corresponds to the phase-separated state (regions II and III in Fig. 2);  $\tau = 0.8$  (1), 0.0 (2),  $-9$  (3).

Line 2 corresponds to the phase transition temperature in the absence of interaction between the charge and the order parameter

The line  $T(\tau_3)$  in Fig. 2 indicates the boundary of the region of an inhomogeneous metastable phase. The inhomogeneous state for the interval  $T(\tau_1) < T < T(\tau_3)$  corresponds to a local free energy minimum but the free energy is positive in this state ( $\Phi > 0$ ), while the homogeneous state has an energy equal to zero. This metastable state is similar to “superheated liquid”.

Fig. 3 shows the phase diagram of the inhomogeneous state in the axes  $x - T$  for the values of the parameters

$$A = 2.5, \quad \frac{\sigma_1 \bar{\rho}}{\alpha' x} = 1200 \text{ K},$$

$$\frac{\tau}{\alpha'} \sqrt{\frac{\beta^3}{\zeta}} = 3 \text{ K}, \quad T_c = 30 \text{ K (with } x = 0).$$

Decreasing  $A$  reduces the region where phase separation is observed.

As mentioned in the Introduction, phase separation is observed in manganites and in high-temperature cuprate superconductors. In this paper we have analyzed, as an example, inhomogeneous phases in manganites where a sequence of phase transitions to inhomogeneous states is observed.

**The  $\text{La}_{1-x}\text{Sr}_x\text{MnO}_3$  system.** Let us analyze this system. For instance, the authors of [19] suggest that the available data indicate an electronic phase-separated regime existing only in the phase diagram region  $0.10 < x < 0.15$  and near the PT from the ferromagnetic to the paramagnetic state.

Let us consider a region above the temperature of the structural PT from a low-temperature pseudocubic phase to an orthorhombic phase or to a Jahn – Teller distorted orthorhombic phase at higher temperatures. Double exchange begins to play a more fundamental role in this region close to structural instability, where long-range Jahn – Teller distortions are suppressed, in the electronic phase-separated regime.

We assume that the following sequence of phase transitions can be observed in this region of the phase diagram with decreasing temperature for the strontium concentration  $x = 0.125$ . First, a transition from homogeneous paramagnetic to inhomogeneous state II occurs at  $T = 184.5 \text{ K}$ . Next, as the temperature decreases, a transition to inhomogeneous



phase III is observed. Finally, only after this, at 155 K, the system undergoes a transition to a uniform ferromagnetic state. This sequence of PTs is very similar to that discussed in our paper. Additionally, such inhomogeneous states may also appear in cuprates.

### Conclusion

We have considered the theory of second-order phase transitions, introducing the Coulomb interaction and charge interaction with the order parameter in addition to the standard expansion of the free energy in powers of the order parameter. We have found the distribution of this parameter and the charge distribution in a 2D plane, which corresponds to a minimum of free energy. We have carried out numerical calculations using the CGM method.

The calculations have confirmed that a region with inhomogeneous distribution of the order parameter and inhomogeneous charge distribution exists between the regions of the

phase diagram characterized by constant values of the order parameter. This phase separation can exist in the form of one-dimensional stripes or two-dimensional rings or “snakes”. A series of phase transitions have been found. A phase transition from a homogeneous state with a zero order parameter to a phase-separated state with two phases (with zero and nonzero order parameters) first occurred as the temperature decreased. Next, a first-order phase transition to another phase-separated state was observed, where both phases had different nonzero values of the order parameter. A transition to a homogeneous ordered state occurred only with a further decrease in temperature.

We have determined the regions in the “temperature – doping level” parameter space where the phases coexist. We have traced the changes in the type of the phase separation depending on the changes in temperature, doping level of the material, and in the coupling constant.

### REFERENCES

- [1] **S. Jin, T.H. Tiefel, M. McCormack, et al.**, Thousandfold change in resistivity in magnetoresistive La-Ca-Mn-O films, *Science*. 264 (5157) (1994) 413–415.
- [2] **M.Yu. Kagan, K.I. Kugel**, Inhomogeneous charge distributions and phase separation in manganites, *Phys. Usp.* 44 (6) (2001) 553–570.
- [3] **A.O. Sboychakov, K.I. Kugel, A.L. Rakhmanov**, Jahn-Teller distortions and phase separation in doped manganites, *Phys. Rev. B*. 74 (1) (2006) 014401(1–13).
- [4] **E. Dagotto, T. Hotta, A. Moreo**, Colossal magnetoresistant materials: the key role of phase separation, *Phys. Rep.* 344 (1–3) (2001) 1–153.
- [5] **E.L. Nagaev**, Lanthanum manganites and other giant-magnetoresistance magnetic conductors, *Phys. Usp.* 39 (8) (1996) 781–805.
- [6] **K.M. Shen, F. Ronning, D.H. Lu, et al.**, Nodal quasiparticles and antinodal charge ordering in  $\text{Ca}_{2-x}\text{Na}_x\text{CuO}_2\text{Cl}_2$ , *Science*. 307 (5711) (2005) 901–904.
- [7] **J.M. Tranquada, H. Woo, T.G. Perring, et al.**, Quantum magnetic excitations from stripes in copper oxide superconductors, *Nature (London)*. 429 (6991) (2004) 534–538.
- [8] **J. Deisenhofer, D. Braak, H.-A. Krug von Nidda, et al.**, Observation of a Griffith’s phase in paramagnetic  $\text{La}_{1-x}\text{Sr}_x\text{MnO}_3$ , *Phys. Rev. Lett.* 95 (25) (2005) 257202(1–4).
- [9] **E.H. Neto da S., P. Aynajian, A. Frano, et al.**, Ubiquitous interplay between charge ordering and high-temperature superconductivity in cuprates, *Science*. 343 (6169) (2014) 393–396.
- [10] **V.V. Kabanov, R.F. Mamin, T.S. Shaposhnikova**, Localized charge inhomogeneities and phase separation near a second-order phase transition, *Sov. Phys. JETP*. 108 (2) (2009) 286–291.
- [11] **V.B. Shenoy, T. Gupta, H.R. Krishnamurthy, T.V. Ramakrishnan**, Coulomb interactions and nanoscale electronic inhomogeneities in manganites, *Phys. Rev. Lett.* 98 (9) (2007) 097201(1–4).
- [12] **J. Miranda, V.V. Kabanov**, Coulomb frustrated first order phase transition and stripes, *Physica C*. 468 (4) (2008) 358–361.
- [13] **C. Ortix, J. Lorenzana, C. Di Castro**, Coarse grained models in Coulomb frustrated phase separation, *J. Phys.: Condens. Matter*. 20 (43) (2008) 434229 (1–8).
- [14] **R. Jamei, S. Kivelson, B. Spivak**, Universal aspects of Coulomb-frustrated phase separation, *Phys. Rev. Lett.* 94 (5) (2005) 056805(1–4).
- [15] **R.F. Mamin, T.S. Shaposhnikova, V.V. Kabanov**, Phase separation and second-order phase transition in the phenomenological model for a Coulomb-frustrated two-dimensional system, *Phys. Rev. B*. 2018. Vol. 97 (9) (2018) 094415(1–7).
- [16] **P.-G. de Gennes**, Effects of double

exchange in magnetic crystals, Phys. Rev. 118 (1) (1960) 141–154.

[17] **Yu.A. Izyumov, Yu.N. Skryabin**, Double exchange model and the unique properties of the manganites, Phys. Usp. 2001. Vol. 44. No. 2. Pp. 109–134.

[18] **C. Zener**, Interaction between the *d*-shells in

the transition metals. II. Ferromagnetic compounds of manganese with perovskite structure, Phys. Rev. 82 (3) (1951) 403–405.

[19] **M. Paraskevopoulos, F. Mayr, J. Hemberger, et al.**, Magnetic properties and the phase diagram of  $\text{La}_{1-x}\text{Sr}_x\text{MnO}_3$  for  $x \leq 0.2$ , J. Phys.: Condens. Matter. 12 (17) (2000) 3993–4011.

*Received 23.05.2018, accepted 24.05.2018.*

#### THE AUTHORS

**SHAPOSHNIKOVA Tatyana S.**

*Zavoisky Physical-Technical Institute, FRC KazanSC of RAS*  
10/7, Sibirsky tract, Kazan, 420029, Russian Federation  
t\_shap@kfti.knc.ru

**MAMIN Rinat F.**

*Zavoisky Physical-Technical Institute, FRC KazanSC of RAS*  
10/7, Sibirsky tract, Kazan, 420029, Russian Federation  
mamin@kfti.knc.ru